JACS
JOURNAL OF THE AMERICAN CHEMICAL SOCIETY
Article
pubs.acs.org/JACS

Spectroscopic Studies of the EutT Adenosyltransferase from *Salmonella enterica*: Mechanism of Four-Coordinate Co(II)Cbl Formation

Ivan G. Pallares,[†] Theodore C. Moore,[‡] Jorge C. Escalante-Semerena,[‡] and Thomas C. Brunold*[,†]

[†]Department of Chemistry, University of Wisconsin—Madison, Madison, Wisconsin 53706, United States
[‡]Department of Microbiology, University of Georgia, Athens, Georgia 30602, United States

Supporting Information

ABSTRACT: EutT from *Salmonella enterica* is a member of a class of enzymes termed ATP:Co(I)rrinoid adenosyltransferases (ACATs), implicated in the biosynthesis of adenosylcobalamin (AdoCbl). In the presence of cosubstrate ATP, ACATs raise the Co(II)/Co(I) reduction potential of their cob(II)alamin [Co(II)-Cbl] substrate by >250 mV via the formation of a unique four-coordinate (4c) Co(II)Cbl species, thereby facilitating the formation of a "supernucleophilic" cob(I)alamin intermediate required for the formation of the AdoCbl product. Previous kinetic studies of EutT revealed the importance of a $HX_{11}CCX_2C(83)$ motif for catalytic activity and have led to the proposal that residues in this motif serve as the binding site for a divalent transition metal cofactor [e.g., Fe(II) or Zn(II)]. This motif is absent in other ACAT families, suggesting that EutT employs a distinct mechanism for AdoCbl formation. To assess how metal ion binding to the $HX_{11}CCX_2C(83)$ motif affects the relative yield of 4c Co(II)Cbl generated in the EutT active site, we have characterized several enzyme variants by using electronic absorption, magnetic circular dichroism, and electron paramagnetic resonance spectroscopies. Our results indicate that Fe(II) or Zn(II) binding to the $HX_{11}CCX_2C(83)$ motif of EutT is required for promoting the formation of 4c Co(II)Cbl. Intriguingly, our spectroscopic data also reveal the presence of an equilibrium between five-coordinate "base-on" and "base-off" Co(II)Cbl species bound to the EutT active site at low ATP concentrations, which shifts in favor of "base-off" Co(II)Cbl in the presence of excess ATP, suggesting that the base-off species serves as a precursor to 4c Co(II)Cbl.

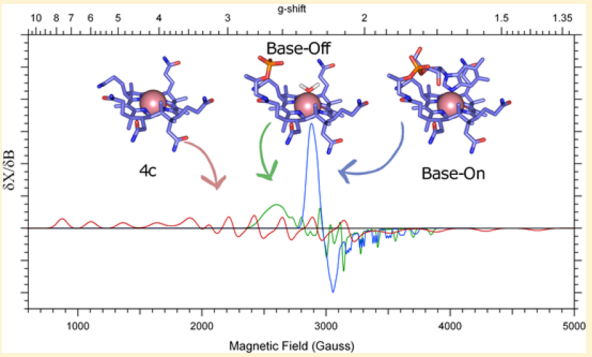

INTRODUCTION

EutT is the most recently identified ATP:Co(I)rrinoid adenosyltransferase (ACAT) enzyme[1,2] involved in maintaining the supply of adenosylcobalamin (AdoCbl) in *Salmonella enterica*.[3] AdoCbl and related corrinoid species are characterized by the presence of a redox-active Co(III) ion that is ligated equatorially by the four nitrogen atoms of a tetrapyrrole macrocycle, termed the corrin ring, and by the 5,6-dimethylbenzimidazole (DMB) base at the end of an intramolecular nucleotide loop in the "lower" axial (Coα) position (Figure 1). Various ligands can occupy the "upper" axial (Coβ) position, with biologically relevant forms containing an adenosyl (AdoCbl), methyl (MeCbl), glutathionyl (GSCbl), or nitrosyl (NOCbl) moiety.[4−6] In the case of AdoCbl, homolytic cleavage of the Co−C(Ado) bond to generate an adenosyl radical and a five-coordinate Co(II)Cbl species with a vacant Coβ position is the first step in reactions catalyzed by AdoCbl-dependent eliminases/mutases.[7] Loss or inactivation of AdoCbl during turnover leads to deactivation of these enzymes, requiring replacement of their cofactor.[8] ACATs are thus implicated in the reactivation of AdoCbl-dependent enzymes, as these adenosyltransferases generate AdoCbl (or coenzyme B_{12}) from ATP and Co(II)Cbl substrates.[3,9]

In *Salmonella enterica*, the *eutT* gene is part of a 16-gene operon, whose expression is triggered by the presence of ethanolamine and adenosylcobalamin (AdoCbl),[10,11] leading to the formation of proteinaceous polyhedron-shaped bodies. These so-called *eut* metabolosomes are postulated to encapsulate the metabolic machinery employed by the cell for the catabolism of ethanolamine.[12,13] The ability of *S. enterica* to use ethanolamine as a source of nutrition was suggested to provide this bacterium with a growth advantage over other intestinal flora under inflammatory conditions,[14] as ethanolamine is readily available in the mammalian gut.[11,15] In this metabolic pathway, the AdoCbl-dependent ethanolamine ammonia lyase (EAL) enzyme (the product of the *eutB* and *eutC* genes) catalyzes the conversion of ethanolamine to acetaldehyde and ammonia.[16] EutT has been postulated to

Received: November 8, 2015
Published: February 17, 2016

ACS Publications © 2016 American Chemical Society

DOI: 10.1021/jacs.5b11708
J. Am. Chem. Soc. 2016, 138, 3694−3704

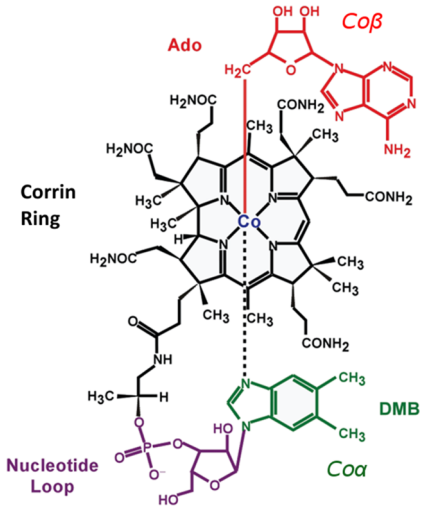

Figure 1. Chemical structure of adenosylcobalamin (AdoCbl), the final product of the reaction catalyzed by ATP:Co(I)rrinoid adenosyltransferases (ACATs).

supply the levels of AdoCbl required for EAL to perform this function.[2,17] Notably, the presence of *eutT* genes was observed to correlate with higher incidence of gastroenteritis.[18]

In addition to EutT, two nonhomologous ACATs are present in *S. enterica*.[3] The *Se*CobA ACAT is continuously produced to maintain basal concentrations of AdoCbl and is involved in the de novo synthesis of AdoCbl and in the scavenging of incomplete corrinoids.[19,20] The gene encoding for *Se*PduO is part of the *pdu* operon that allows *S. enterica* to utilize 1,2-propanediol as a source of carbon and energy. PduO-type enzymes are homologous to the human adenosyltransferase (hATR), which has been shown to deliver its AdoCbl product directly to the B_{12}-dependent methylmalonyl CoA-mutase (MMCM) enzyme.[21,22] Despite the lack of sequence and structural homologies among the known families of ACATs, a common Co−C(Ado) bond formation mechanism has previously been proposed for these enzymes involving the reduction of a Co(II)rrinoid precursor in their active sites to generate a "supernucleophilic" Co(I) species capable of attacking the 5′-carbon of ATP.[3,23,24] A particularly challenging step in this mechanism involves the reduction of Co(II)rrinoids to generate the key Co(I) intermediate, as the reduction potentials of Co(II)rrinoids free in solution are well below those of available reducing agents in the cell (e.g., $E°$(NHE) = −610 mV for Co(II)Cbl and −490 mV for cob(II)inamide [Co(II)Cbi$^+$], a Co(II)Cbl precursor that lacks the nucleotide loop and DMB moiety).[25] However, Co(II)Cbl species bound to the active sites of EutT and the PduO-type ACAT from *Lactobacillus reuteri* (*Lr*PduO) are readily reduced by free dihydroflavins to generate Co(I)Cbl, (e.g., $E°$(NHE) = −228 mV for FMN at pH 7.5)[26,27] or by reduced flavoproteins in the case of *Se*CobA ($E°$(NHE) = −440 mV for the semiquinone/reduced flavin couple of FldA, the purported physiological partner of *Se*CobA).[28−30] Extensive biochemical,[31,32] crystallographic,[32−35] and spectroscopic studies[36−38] of *Se*CobA and different PduO-type ACATs have revealed that a structurally unique four-coordinate (4c) Co(II)Cbl species is generated by these enzymes in the presence of ATP. The most recent X-ray crystal structures reported for *Se*CobA and *Lr*PduO complexed with Co(II)Cbl and MgATP have provided evidence that the DMB moiety that occupies the Co*α* position of Co(II)Cbl in solution is displaced by a noncoordinating phenylalanine residue (F112 in *Lr*PduO and F91 in *Se*CobA). Subsequent electron paramagnetic resonance (EPR) and magnetic circular dichroism (MCD) characterization of Co(II)Cbl in the presence of *Se*CobA and *Lr*PduO identified the roles specific amino acid residues play with regard to the formation of 4c Co(II)Cbl.[38,39] These studies were facilitated by the fact that a sharp feature centered at ∼12 000 cm^{-1} appears in the MCD spectra of Co(II)Cbl bound to *Se*CobA/MgATP and *Lr*PduO/MgATP, whose intensity correlates directly with the relative amount of 4c Co(II)Cbl generated in these enzymes. The appearance of this feature was shown to reflect a sizable stabilization of the singly occupied, redox-active Co $3d_{z^2}$-based molecular orbital in 4c Co(II)Cbl, which was predicted to lead to an increase in the Co(II)/Co(I) reduction potential by ≥250 mV.[24,36,40]

We have recently obtained spectroscopic evidence that also supports the formation of a 4c Co(II)Cbl species in the active site of EutT in the presence of excesss MgATP.[41] Moreover, our data indicated that EutT is unable to generate 4c Co(II)Cbi$^+$, in contrast to the *Se*CobA and PduO-type ACATs. Consistent with this observation, bioassay and kinetic studies revealed that EutT fails to adenosylate this Co(II)Cbl precursor.[41] Because EutT has thus far eluded characterization by X-ray crystallography, the approach by which it binds its Co(II)Cbl substrate and generates 4c Co(II)Cbl remains unknown. Biochemical characterizations of EutT provided evidence that this enzyme exists as a dimer in solution and requires a divalent transition metal cofactor for catalytic activity, in striking contrast to the other known families of ACATs.[27,42] The activity of EutT was found to be highest in the presence of Fe(II) ions under anaerobic conditions, followed by Zn(II) and Co(II) ions, with only the latter two also supporting catalytic activity in the presence of oxygen.[27] Inspection of the primary sequence of EutT led to the proposal that that HX_{11}CCXXC-(83) motif may be involved in divalent metal ion binding, as similar motifs are found in *Bacillus subtilis* CbiX, a 4Fe/4S-containing enzyme, as well as some Zn-finger proteins. Elemental analyses of wild-type EutT (EutT^{WT}) and variants with a single alanine substitution at either the H67, C79, C80, or C83 position confirmed that EutT^{WT} incorporates Fe(II) and Zn(II) ions in an ∼2:1 protein-to-metal ratio, with the EutT^{C80A} and EutT^{C83A} variants exhibiting a dramatically reduced metal ion affinity. Futhermore, the level of metal incorporation into EutT^{WT} and the alanine variants was found to correlate directly with enzymatic activity.[41]

To obtain further insight into the roles played by the divalent metal cofactor of EutT with respect to the formation of 4c Co(II)Cbl, we have employed MCD and EPR spectroscopies to probe the interaction of Co(II)Cbl with EutT^{WT} containing either Fe(II) [EutT^{WT}/Fe] or Zn(II) [EutT^{WT}/Zn] as well as variants possessing a single alanine substitution at the H67, H75, C79, C80, or C83 position. These techniques offer a uniquely sensitive probe of changes in the coordination environment of the cobalt ion as Co(II)Cbl binds to the EutT active site. While MCD spectroscopy allows for the identification of ligand field (LF) and charge transfer (CT) transitions, whose energies are substantially different for 4c and five-coordinate (5c) Co(II)Cbl, EPR spectroscopy provides a complementary probe of the 5c "base-on" (DMB bound) and "base-off" (water bound) fractions of Co(II)Cbl generated in the EutT active site. Collectively, these techniques have enabled us to determine how the relative populations of 4c and 5c

DOI: 10.1021/jacs.5b11708
J. Am. Chem. Soc. 2016, 138, 3694−3704

Co(II)Cbl species generated in the EutT^{WT} active site are affected by divalent metal ion incorporation and amino acid substitutions in the $HX_{11}CCX_2C(83)$ motif. The results obtained in this study provide unprecedented insight into the mechanism employed by EutT to generate AdoCbl.

METHODS

Cofactors and Chemicals. The chloride salt of aquacobalamin ([H_2OCbl]Cl) and potassium formate (HCOOK) were purchased from Sigma and used as obtained. Co(II)Cbl was generated by addition of a small amount (~40 μL) of saturated HCOOK solution to a degassed sample (0.5 mL) of aqueous H_2OCbl^+ (~5 mM) in a sealed vial. The progress of the reduction was monitored spectrophotometrically. The magnesium salt of ATP was used throughout all experiments.

Protein Preparation and Purification. EutT production and purification was performed as described elsewhere.[27] Briefly, EutT from *Salmonella enterica* sv. Typhimurium LT2 (EutT) was overexpressed from a pTEV6 vector in *Escherichia coli* BL21, which generated a fusion protein with cleavable *N*-terminal hexahistidine (H_6) and maltose binding protein (MBP) tags. EutT variants were generated using the QuikChange II site-directed mutagenesis kit (Stratagene). All proteins were purified on a HisTrap nickel-affinity column (GE Healthcare). The H_6-MBP tag was cleaved using recombinant tobacco-etch protease (rTEV).[43] The tag was separated from the protein using a HisTrap nickel-affinity column and an amylose column (New England Biolabs).

To prepare samples of metalated EutT for spectroscopic studies, the protein was concentrated to a least 25 mg/mL (Amicon Ultra, 10 000 MWCO). EutT was placed into dialysis units (D-tube mini, Novagen) and moved into an anoxic chamber. The EutT solution was then dialyzed three times for 30 min against 1.0 L of degassed buffer (2-[4-(2-hydroxyethyl)piperazin-1-yl]ethanesulfonic acid (HEPES, 50 mM, pH 7) containing NaCl (300 mM), tris(2-carboxyethyl)phosphine (TCEP, 0.25 mM), ethylenediaminetetraacetic acid (EDTA, 2 mM), and low (10 μM) or high (1 mM) concentrations of MgATP). To generate EutT/Fe, ApoEutT samples were dialyzed against chelex-treated buffer containing $FeSO_4$ (1 mM) and low or high MgATP (3 × 1L, 30 min each). Since recombinant EutT copurifies with zinc,[27] EutT/Zn was instead prepared by dialysis against chelex-treated buffer devoid of EDTA, but containing low or high concentrations of MgATP (3 × 1L, 30 min each). Metalated EutT samples were gently resuspended with 100% glycerol to a final concentration of 10 mg/mL and 60% glycerol. Samples were stored in airtight serum vials (Wheaton) and flash-frozen in liquid nitrogen until use.

Sample Preparation. Purified EutT (~300−600 μM) in HEPES buffer (50 mM, pH 7) containing NaCl (300 mM) and TCEP (0.25 mM) was incubated with Co(II)Cbl under anoxic conditions. To generate EutT samples in the presence of excess MgATP, ~ 10 μL of a concentrated MgATP solution were added to yield a final MgATP concentration of >5 mM. Further details of sample compositions are provided in Table S1. Protein solutions were injected into the appropriate sample cells in an oxygen-free chamber. Following removal from the anoxic chamber, the samples were frozen and stored in liquid nitrogen. For the MCD samples, room temperature absorption (Abs) spectra were collected under an N_2 atmosphere before they were frozen. No changes in the Abs spectrum of Co(II)Cbl due to oxidation or sample degradation were observed after freezing the samples.

Spectroscopy. MCD and low-temperature Abs spectra were collected on a Jasco J-715 spectropolarimeter in conjunction with an Oxford Instruments SM-4000 8T magnetocryostat. All MCD spectra presented herein were obtained by taking the difference between spectra collected with the magnetic field oriented parallel and antiparallel to the light propagation axis to remove contributions from the natural CD and glass strain. X-band EPR spectra were obtained by using a Bruker ESP 300E spectrometer in conjunction with an Oxford ESR 900 continuous-flow liquid helium cryostat and an Oxford ITC4 temperature controller. The microwave frequency was measured with a Varian EIP model 625A CW frequency counter. All spectra were collected using a modulation amplitude of 10 G and a modulation frequency of 100 kHz. EPR spectral simulations were performed using Dr. Mark Nilges's SIMPOW program.[44]

RESULTS

Effect of Metal Substitution on 4c Co(II)Cbl Formation. To determine how the identity of the divalent metal ion cofactor affects the binding of Co(II)Cbl to EutT, we collected low-temperature Abs and MCD data of Co(II)Cbl in the absence and presence of enzyme and cosubstrate ATP. In the Abs spectrum of Co(II)Cbl obtained in the absence of EutT (Figure 2C), an intense feature is observed at 21 000 cm^{-1} (the so-called α-band) that has previously been attributed

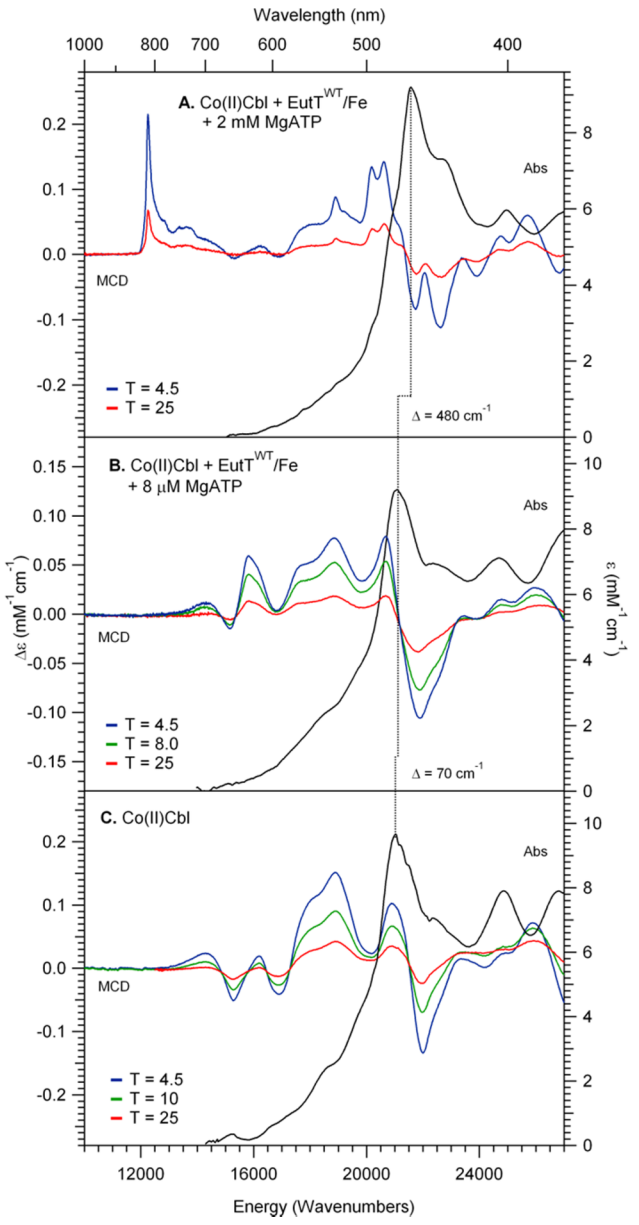

Figure 2. Abs spectra collected at 4.5 K (black traces) and 7 T VT-MCD spectra of (A) Co(II)Cbl in the presence of EutT^{WT}/Fe and a large molar excess (2 mM) of MgATP, (B) Co(II)Cbl in the presence of EutT^{WT}/Fe and substoichiometric (8 μL) MgATP, and (C) free Co(II)Cbl. The dashed vertical line position of the α-band in the Abs spectra.

DOI: 10.1021/jacs.5b11708
J. Am. Chem. Soc. 2016, 138, 3694−3704

Table 1. Positions of the δ-Band (MCD) and the α-Band (Abs) of 4c Co(II)Cbl Species Generated in the Active Site of EutT^{WT} and Several Variants[a]

		Co(II)Cbl				
metal present	*Se*EutT substitution	$\nu(\delta)$/cm^{-1}	$\Delta\nu(\delta)$/cm^{-1}	$\nu(\alpha)$/cm^{-1}	$\Delta\nu(\alpha)$/cm^{-1}	4c-Cbl yield/%
Zn(II)	none (WT), >10× MgATP	12 277	22	21 645	615	>95
	none (WT)	12 217	−38	21 552	522	81
	none (WT), no TCEP	12 225	−30	21 551	521	71
Fe(II)	none (WT)	12 255	0	21 575	545	>95
	C79A	12 232	−23	21 505	475	46
	H75A	12 195	−60	21 164	134	26
	H67A	12 195	−60	21 030	0	12
	C80A	n/a	n/a	21 142	112	n/d
	C83A	n/a	n/a	21 053	23	n/d

[a]Shifts in the δ-band are shown relative to the position of this feature in the MCD spectrum of Co(II)Cbl in the presence of EutT^{WT}/Fe and excess MgATP. Also shown are the relative yields of 4c Co(II)Cbl species estimated from the δ-band intensities. Shifts in the α-band are shown relative to the position of this feature in the Abs spectrum of Co(II)Cbl in the absence of ACATs (λ_{max} = 475 nm).

to the lowest-energy corrin $\pi \rightarrow \pi^*$ transition on the basis of its high intensity and TDDFT calculations.[7,45] The prominent shoulder on the low energy side of the α-band was assigned to metal-to-ligand charge transfer (MLCT) transitions,[7,45] while the intense, sharp feature peaking at 32 000 cm^{-1} was attributed to another corrin $\pi \rightarrow \pi^*$ transition. Upon the addition of wild-type EutT metalated with Fe(II) ions (EutT^{WT}/Fe) and substochiometric amounts (<10 μM) of MgATP to a solution of Co(II)Cbl, the intensity of this near-UV Abs band decreases by ∼30% (Figure S7), consistent with substrate Co(II)Cbl binding to the enzyme active site (vide infra). In the presence of EutT^{WT}/Fe and an ∼10-fold molar excess of MgATP (EutT^{WT}/Fe + MgATP), a similar decrease in the intensity of this Abs feature is observed, along with an ∼550 cm^{-1} blue-shift of the α-band (Figure 2A). In previous studies of Co(II)Cbl in the presence of *Se*CobA or *Lr*PduO, a sizable blue-shift of the α-band was shown to reflect the formation of a 4c Co(II)Cbl species in the enzyme active site.[36,37] Intriguingly, the shift of the α-band of Co(II)Cbl caused by the addition of EutT^{WT}/Fe + MgATP is ∼150 cm^{-1} larger than that induced by the addition of *Se*CobA or *Lr*PduO and MgATP.[36−38]

The MCD spectrum of Co(II)Cbl in the absence of EutT is characterized by a series of derivative-shaped features that give rise to the appearance of four oppositely signed bands centered at ∼16 000 cm^{-1}, as well as additional, positively signed bands around 19 000 cm^{-1} (Figure 2C).[7] The two lowest-energy features in this spectrum have previously been assigned to LF transitions primarily involving electronic excitations from the doubly occupied Co 3d$_{xz}$- and 3d$_{yz}$-based molecular orbitals (MOs) to the singly occupied Co 3d$_{z^2}$-based MO.[46] Additional features between 16 000 and 22 000 cm^{-1} have generally been attributed to metal-to-ligand charge transfer (MLCT) or additional LF transitions, with specific assignments made difficult by the presence of multiple transitions with similar energies in this region.

The MCD spectrum of Co(II)Cbl in the presence of EutT^{WT}/Fe exposed to oxygen is nearly superimposable on that of Co(II)Cbl free in solution (Figure S1, bottom). Likewise, only minor spectral differences are observed between the corresponding Abs spectra (Figure S1, top). These results suggest that Co(II)Cbl does not bind to EutT^{WT}/Fe under aerobic conditions, in support of our proposal that the Fe(II) ion of EutT^{WT}/Fe is susceptible to air oxidation and that the Fe(III) ion formed in this process is released from the protein.[27] In contrast, the MCD spectrum of an anaerobic sample of Co(II)Cbl in the presence of EutT^{WT}/Fe and a substoichiometric (∼10 μM) amount of MgATP to enhance protein stability[27] exhibits unique features in the 14 000−22 000 cm^{-1} region (Figure 2B). Most notably, the positive features at ∼16 000 and ∼21 000 cm^{-1} in the MCD spectrum of free Co(II)Cbl (Figure 2C) red-shift by ∼500 and ∼400 cm^{-1}, respectively, in the presence of EutT^{WT}/Fe (Figure 2B), which could potentially reflect the formation of base-off Co(II)Cbl (vide infra). The corresponding Abs spectrum reveals that the α-band does not actually red-shift in the presence of EutT^{WT}, suggesting that the MCD feature at 21 000 cm^{-1} arises from one of the many CT transitions of Co(II)Cbl whose energies are expected to be particularly sensitive to changes in the local environment of Co(II)Cbl. Further changes in the relative intensities and bandwidths of features that occur in this region of the MCD spectrum provide additional evidence that a significant fraction of Co(II)Cbl binds to the EutT^{WT}/Fe active site in the absence of cosubstrate MgATP.

The low-energy region of the MCD spectrum of Co(II)Cbl in the presence of EutT^{WT}/Fe and a large (>10-fold) molar excess of MgATP is characterized by an intense, positively signed sharp feature at ∼12 300 cm^{-1} (δ-band) and a broad band at ∼13 600 cm^{-1} (β-band) (Figure 2A). These features, which have previously been assigned to the electronic origin and a vibrational sideband of the Co 3d$_{x^2-z^2}$ → 3d$_{z^2}$ LF transition, are characteristic of 4c Co(II)rrinoids generated in the active sites of ACATs via elimination of any axial ligand interactions.[36,38−41] The relative MCD intensities of the δ-band associated with 4c Co(II)Cbl and features originating from 5c Co(II)Cbl indicate that >95% of the Co(II)Cbl substrate was converted to a 4c species in this sample (Table 1). Consistent with this high 5c → 4c conversion yield, additional spectroscopic features from 4c Co(II)Cbl are clearly observed at ∼20 000 cm^{-1}, termed the λ- and σ-bands (Figure S2), which are usually masked by more intense contributions from the remaining 5c Co(II)Cbl species. The 5c → 4c Co(II)Cbl conversion yield achieved by EutT^{WT}/Fe in the presence of excess MgATP largely exceeds the conversion yields reported for *Se*CobA and *Lr*PduO under similar conditions (∼8% and 40%, respectively).[38,39]

The Abs and MCD spectra of Co(II)Cbl in the presence of EutT^{WT}/Fe and its metal-substituted EutT^{WT}/Zn derivative are nearly indistinguishable from each other (as well as the Abs and MCD spectra of Co(II)Cbl in the presence of EutT^{WT}/Zn

DOI: 10.1021/jacs.5b11708
J. Am. Chem. Soc. 2016, 138, 3694−3704

published previously[41]) under both minimal and excess MgATP conditions (Figure S2), indicating that the Fe(II)- and Zn(II)-bound forms of EutT^{WT} possess very similar Co(II)Cbl binding sites. The 5c → 4c Co(II)Cbl conversion yield in the presence of EutT^{WT}/Zn and a 3-fold excess of MgATP is ∼81%, which is somewhat lower than that obtained with EutT^{WT}/Fe under similar conditions (Table 1). However, in the presence of ∼5 mM MgATP (a >10-fold molar excess of MgATP over EutT), the 5c → 4c Co(II)Cbl conversion of EutT^{WT}/Zn becomes analogous to that of EutT^{WT}/Fe (Table 1). Even though EutT^{WT}/Zn is stable in air (in contrast to EutT^{WT}/Fe), a small (∼10%) decrease in the 5c → 4c Co(II)Cbl conversion yield is noted in the absence of TCEP, possibly due to partial oxidation of the Cys residues (Table 1).

Because the identity of the divalent metal ion that is present in EutT^{WT} in vivo is currently unknown, these findings clearly warrant further spectroscopic studies of both EutT^{WT}/Fe and EutT^{WT}/Zn. Given that EutT^{WT} is active with Fe(II) and Zn(II), it is obvious that the divalent metal ion primarily plays a structural role. However, circular dichroism (CD) studies of EutT in the absence and presence of divalent metal ions did not reveal any significant conformational differences between the two enzyme forms, suggesting that the metal binding site encompasses a relatively small portion of the protein fold.[27]

Effect of Cosubstrate MgATP Concentration on the 5c → 4c Co(II)Cbl Conversion Yield. Because the single unpaired electron of Co(II)Cbl resides in the Co $3d_{z^2}$-based MO, electron paramagnetic resonance (EPR) spectroscopy provides an extremely sensitive probe of perturbations to the axial ligand of Co(II)Cbl by the protein environment. At low MgATP concentration (∼10 μM), a broad positive feature around 2620 G can be clearly discerned in the EPR spectrum of Co(II)Cbl in the presence of EutT^{WT}/Fe (Figure 3B). This feature is notably absent in the EPR spectrum of base-on Co(II)Cbl (Figure 3A), which lacks any visible features below 2800 G; rather, it is characteristic of a base-off species in which the DMB ligand has been replaced by a solvent-derived water molecule (Figure 3E). The presence of partially resolved hyperfine structure on the 2620 G feature suggests that the enzyme active site imposes conformational constraints on the Co(II)Cbl substrate even in the absence of MgATP. While both base-off and base-on Co(II)Cbl contribute to the region of the EPR spectrum above 2800 G, the presence of an intense derivative-shaped feature centered at 2950 G and peak splittings near ∼3350 G due to ^{14}N (I = 1) superhyperfine coupling are a clear indication of DMB coordination to the Co(II) ion. From the relative intensities of these features, we estimate that ∼60% of the Co(II)Cbl substrate is present in the base-off conformation, while the remaining ∼40% is in the base-on conformation. The presence of sharp features in the 3000 G region of the EPR spectrum suggests that the DMB moiety of base-on Co(II)Cbl is conformationally constrained and thus bound to the active site EutT^{WT}/Fe, as these features are absent in the EPR spectrum of free Co(II)Cbl and cannot be attributed to the presence of base-off Co(II)Cbl (vide infra).

Upon the addition of at least a 3-fold molar excess (∼1 mM) of MgATP, a series of weak, derivative-shaped features appear in the 1900−2450 G region of the EPR spectrum of Co(II)Cbl in the presence of EutT^{WT}/Fe (Figure 3C). These broad features are characteristic of square planar, low-spin Co(II) species, consistent with the formation of 4c Co(II)Cbl in the active site of EutT^{WT}/Fe, as observed previously for other ACATs.[36,37,47] In the presence of a > 10-fold molar excess of

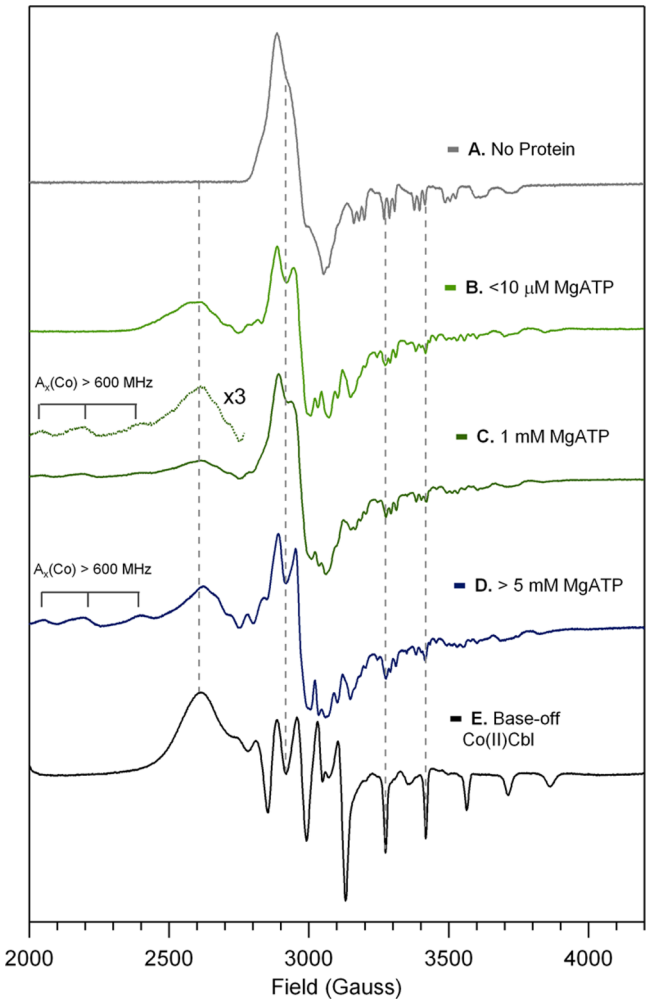

Figure 3. Experimental X-band EPR spectra collected at 20 K of (A) free Co(II)Cbl, (B) Co(II)Cbl in the presence of EutT^{WT}/Fe and minimal (<10 μM) MgATP, and (C) Co(II)Cbl in the presence of EutT^{WT}/Fe with 3-fold molar excess of MgATP, and (D) a >10-fold excess of MgATP. The spectrum of Co(II)Cbi$^+$ (E), a base-off Co(II)Cbl analogue is shown for comparison. EPR spectra were collected using a 9.36 GHz microwave source, 2 mW microwave power, 5 G modulation amplitude, 100 kHz modulation frequency, and a 328 ms time constant. Features from base-off Co(II)Cbl are highlighted with vertical dashed lines. Features from 4c Co(II)Cbl species at low magnetic fields are noted.

MgATP, the features from 4c Co(II)Cbl gain intensity at the expense of those associated with 5c base-on and base-off Co(II)Cbl, indicating an increase in the 5c → 4c Co(II)Cbl conversion yield (Figure 3D). Thus, excess MgATP appears to facilitate the formation of 4c Co(II)Cbl by promoting DMB dissociation to generate 5c base-off Co(II)Cbl and/or by stabilizing the 4c Co(II)Cbl species formed in the active site. While additional features below 1900 G should be observed in the EPR spectrum of 4c Co(II)Cbl in the presence of EutT^{WT}/Fe, these features are masked by intense signals from a ferric minority species in the sample (characteristic derivatives-shaped feature at ∼1600 G, Figure S3).

As in the case of EutT^{WT}/Fe, the EPR spectrum of Co(II)Cbl in the presence of EutT^{WT}/Zn and substoiochiometric (∼10 μM) MgATP exhibits features consistent with the presence of both base-on and base-off Co(II)Cbl (Figures 4 and 5B). Although this spectrum is qualitatively similar to that

DOI: 10.1021/jacs.5b11708
J. Am. Chem. Soc. 2016, 138, 3694−3704

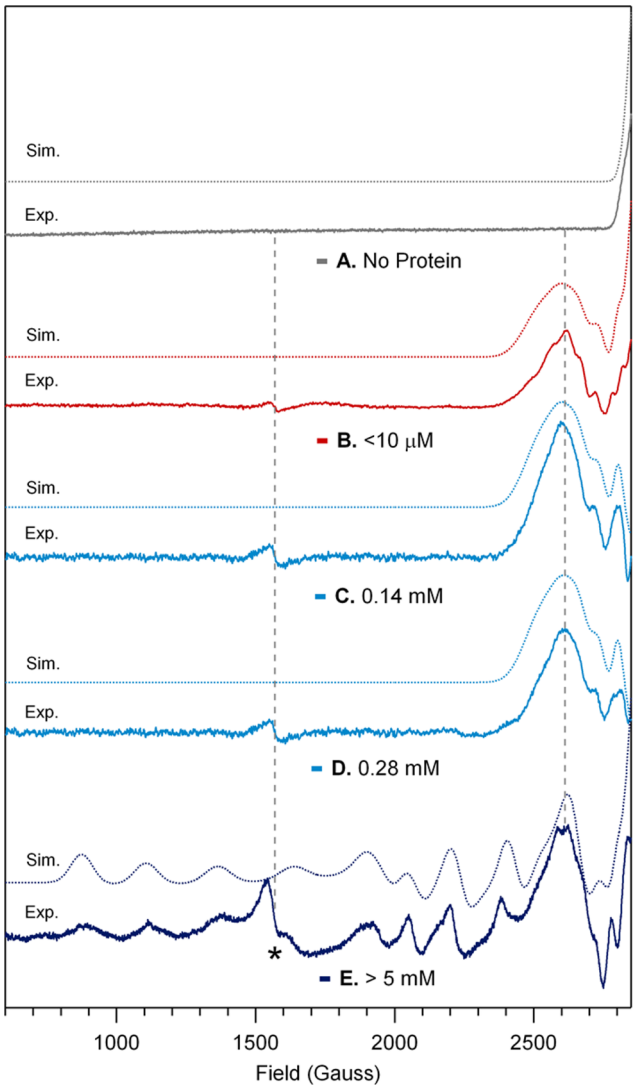

Figure 4. Low-field region of X-band EPR spectra collected at 20 K of (A) free Co(II)Cbl, (B) Co(II)Cbl in the presence of EutT^{WT}/Zn and <10 μM MgATP, and (C) Co(II)Cbl in the presence of EutT^{WT}/Zn and a substoichiometric amount of MgATP, (D) an equimolar amount of MgATP, and (E) a 10-fold molar excess of MgATP. The prominent feature from base-off Co(II)Cbl is highlighted by a vertical line, and the feature arising from ferric impurities is marked by an asterisk. EPR spectra were collected using a 9.36 GHz microwave source, 2 mW microwave power, 5 G modulation amplitude, 100 kHz modulation frequency, and a 328 ms time constant. Spectra were simulated using the parameters provided in Table 2.

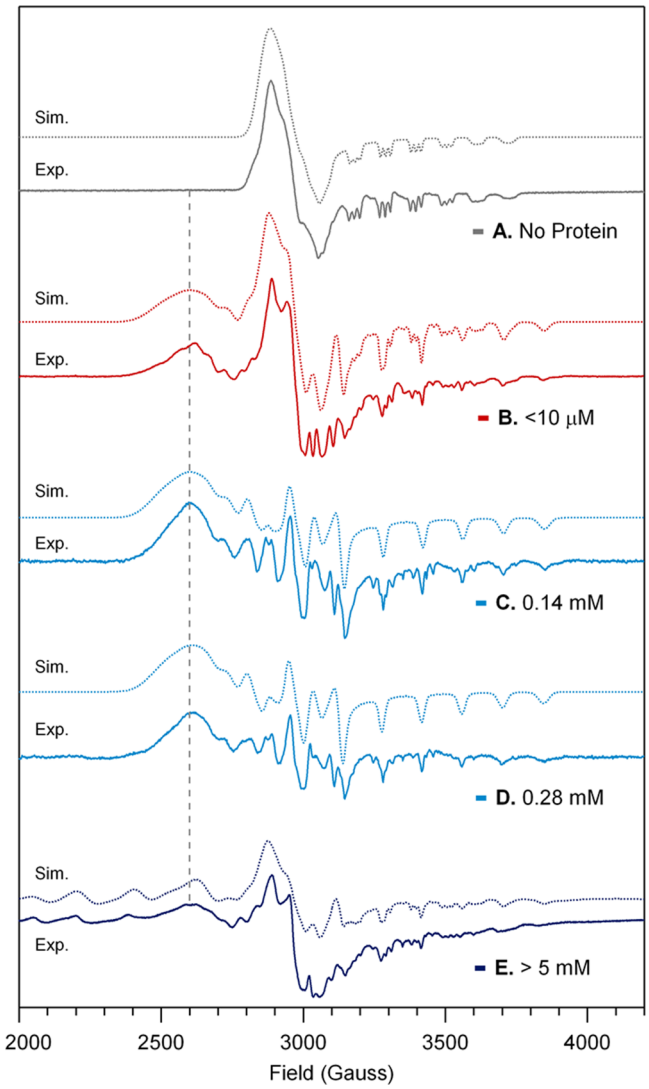

Figure 5. High-field region of X-band EPR spectra collected at 20 K of (A) free Co(II)Cbl, (B) Co(II)Cbl in the presence of EutT^{WT}/Zn and <10 μM MgATP, and (C) in the presence of EutT^{WT}/Zn and a substoichiometric amount of MgATP, (D) an equimolar amount of MgATP, and (E) a 10-fold molar excess of MgATP. The prominent feature from base-off Co(II)Cbl is highlighted by a vertical line. See Figure 4 caption for instrument settings. Spectra were simulated using the parameters provided in Table 2.

obtained in the presence of EutT^{WT}/Fe under similar conditions (Figure S3), ruling out any strong magnetic interactions between the Fe(II) and Co(II) ions in Co(II)-Cbl-bound EutT^{WT}/Fe and thus indicating that the metal ions are separated by at least 10 Å, it is better resolved and thus provides more compelling evidence for the presence of a unique base-off Co(II)Cbl species and of perturbed base-on Co(II)Cbl. Intriguingly, in the presence of EutT^{WT}/Zn and half-molar to equimolar amounts of MgATP, the EPR spectra lack any features from base-on Co(II)Cbl (Figures 4 and 5C, D). Instead, these spectra are very similar to that obtained for Co(II)Cbi$^+$ free in solution (Figure 3E), indicating that under these conditions the Co(II)Cbl substrate is bound to EutT^{WT}/Zn in a base-off conformation. Note that no spectroscopic features from base-on or 4c Co(II)Cbl are discernible in these spectra. A fit of these spectra yields spin-Hamiltonian parameters essentially identical to those obtained for free Co(II)Cbi$^+$ (Table 2), with the exception of a 15−20 MHz smaller A_z(Co) hyperfine coupling constant. Since A_z(Co) correlates with the covalency of the Co−O(H_2) bond (i.e., it decreases as covalency increases), this observation indicates that the water molecule coordinated to the base-off Co(II)Cbl species in EutT^{WT}/Zn forms a more covalent bond with the Co(II) ion than does the axially bound water molecule in Co(II)Cbi$^+$. This finding suggests that the Co−O(H_2) bond is slightly compressed in the EutT^{WT}/Zn active site, thus implying that the α-face of the corrin ring does not become completely exposed to solvent upon DMB dissociation.

In the presence of a 10-fold molar excess of MgATP, the EPR spectrum of Co(II)Cbl with EutT^{WT}/Zn exhibits sharp features between 800 and 1900 G (Figures 4 and 5E), as

DOI: 10.1021/jacs.5b11708
J. Am. Chem. Soc. 2016, 138, 3694−3704

Table 2. Spin-Hamiltonian Parameters for Co(II)Cbl in the Absence and Presence of EutT^{WT} and MgATP[a]

			g-values			A(^{59}Co)/MHz			A(^{14}N)/MHz
		% cont	g_z	g_y	g_x	A_z	A_y	A_x	A(iso)
(A) Co(II)Cbl	base-on	100	2.004	2.232	2.269	303	30	40	49
(B) Co(II)Cbl/EutT^{WT}(Zn)/minimal MgATP	base-on	38	2.004	2.232	2.269	303	30	40	49
	base-off	62	1.991	2.315	2.459	387	222	227	n/a[b]
(C) Co(II)Cbl/EutT^{WT}(Zn)/0.5-fold MgATP	base-off	100	1.991	2.315	2.459	387	222	227	n/a[b]
(D) Co(II)Cbl/EutT^{WT}(Zn)/equimolar MgATP	base-off	100	1.993	2.313	2.459	389	217	224	n/a[b]
(E) Co(II)Cbl/EutT^{WT}(Zn)/>10-fold excess MgATP	base-on	19	2.004	2.232	2.269	303	30	40	49
	base-off	23	1.991	2.315	2.459	387	222	227	n/a[b]
	4c	58	1.800	2.553	3.610	760	625	1362	n/a[b]
(F) Co(II)Cbi$^+$	base-off	100	1.994	2.314	2.423	402	210	226	n/a[b]
(G) Co(II)Cbl/*Lr*PduO/MgATP	4c	n/a[b]	1.900	2.700	2.720	770	755	595	n/a[b]
(H) Co(II)Cbi$^+$/*Se*CobA/MgATP	4c	n/a[b]	2.060	2.670	2.730	805	590	635	n/a[b]

[a]Parameters for 4c Co(II)rrinoids generated by *Se*CobA and *Lr*PduO from refs 36 and 37 are shown for comparison (G and H). [b]Not applicable.

reported previously.[41] These features are identical to those displayed by 4c Co(II)Cbl bound to EutT^{WT}/Fe + MgATP, but the minuscule amount of Fe(III) in our EutT^{WT}/Zn samples allows for the observation of additional peaks at lower fields. A fit of this spectrum yields *g*-shifts and *A*(Co) values (Table 2E) that are significantly larger than those reported for the 4c Co(II)rrinoids generated in the active site of the other ACATs (Table 2G and H). The increased rhombicity of the g-tensor (resulting in $g_x > g_y > g_z$) is noteworthy, as the magnitudes of the *g*-shifts are sensitive to the conformation of 4c Co(II)-rrinoids. Particularly intriguing are the very large values obtained for g_x and A_x(Co) (3.61 and 1362 MHz, respectively). These values suggest that the conformation of the 4c Co(II)Cbl species in EutT is substantially different from that adopted in the other ACATs.[33,34]

Consistent with the findings summarized above, the MCD spectrum of Co(II)Cbl in the presence of EutT^{WT}/Zn and an approximately equimolar amount of MgATP is dominated by a base-off Co(II)Cbl species that is generated in the enzyme active site (Figure 6C). Intriguingly, this spectrum is not superimposable on that of Co(II)Cbi$^+$, as the features near 16 000 and 21 000 cm^{-1} are red-shifted by ~500 and ~300 cm^{-1}, respectively, in the spectrum of the enzyme-bound base-off Co(II)Cbl species (Figure 6E). These shifts are very similar to those observed for Co(II)Cbl in the presence of EutT^{WT}/Zn and substoichiometric MgATP (Figure 6D). Based on our EPR results, these changes can be attributed to the formation of a slightly perturbed base-off Co(II)Cbl species in the active site of EutT^{WT}/Zn. Addition of a 10-fold molar excess of MgATP to a sample of Co(II)Cbl in the presence of EutT^{WT}/Zn and equimolar MgATP leads to the appearance of an MCD spectrum that is dominated by contributions from a 4c Co(II)Cbl species (Figure 6B) and nearly indistinguishable from that obtained with EutT^{WT}/Zn purified in the presence of a large (~10-fold) molar excess MgATP (Figure 6, A). This observation suggests that the base-off Co(II)Cbl generated in EutT^{WT} is a possible intermediate in the formation of 4c Co(II)Cbl. This unique base-off Co(II)Cbl species is present in the active site of EutT^{WT}/Zn even under low MgATP conditions (i.e., >30-fold Co(II)Cbl:MgATP molar excess), indicating that MgATP does not have to be present in the active site before the enzyme can bind Co(II)Cbl and displace its DMB moiety.

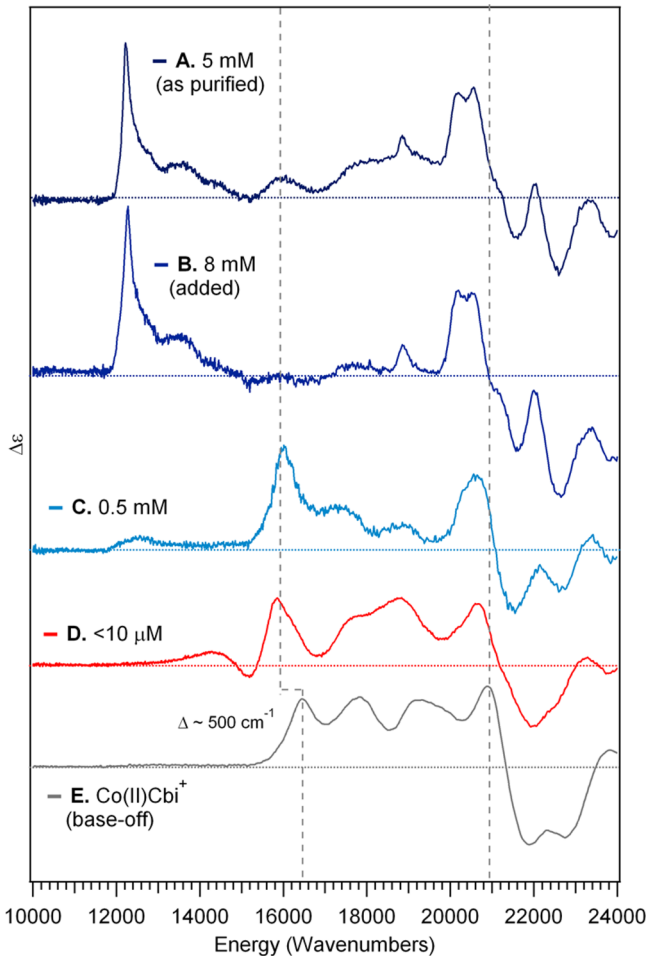

Figure 6. MCD spectra of Co(II)Cbl obtained in the presence of EutT^{WT}/Zn and various MgATP concentrations. (A) ~5 mM MgATP (~10-fold molar excess), (C) equimolar amounts of MgATP and EutT, and (D) substoichiometric (<10 μM) MgATP. Trace (B) was obtained after the addition of MgATP to the sample used in (C) to increase the concentration to ~8 mM (>10-fold excess). The MCD spectrum of Co(II)Cbi$^+$ (E), a base-off Co(II)Cbl analogue, is shown for comparison. Primary spectroscopic features of this species are highlighted by dashed vertical lines.

Effect of Amino Acid Substitutions on 4c Co(II)Cbl Formation. The activity of EutT^{WT} and selected variants has previously been shown to correlate with the degree of Fe(II) or Zn(II) incorporation into the enzyme. The C79, C80, C83, and H67 residues that are part of the conserved $HX_{11}CCX_2C(83)$ motif of EutT^{WT} were found to be particularly important for

DOI: 10.1021/jacs.5b11708
J. Am. Chem. Soc. 2016, 138, 3694−3704

the binding of divalent transition metal ions, as variants containing alanine substitutions at these positions displayed significantly lower metalation levels than the wild-type enzyme.[27] Because the three-dimensional structure of EutT^{WT} has yet to be determined, the nature of the divalent metal ion binding site and the mechanism by which metal incorporation into the $HX_{11}CCX_2C(83)$ motif modulates the catalytic activity of EutT^{WT} are currently unknown. In order to address this issue, we studied the effects of alanine substitutions within this motif on the binding of Co(II)Cbl to EutT/Fe and the yield of 4c Co(II)Cbl species.

The MCD spectra of Co(II)Cbl in the presence of EutT/Fe variants possessing a single alanine substitution at either the H67, H75, C79, C80, or C83 position are show in Figure 7 (the

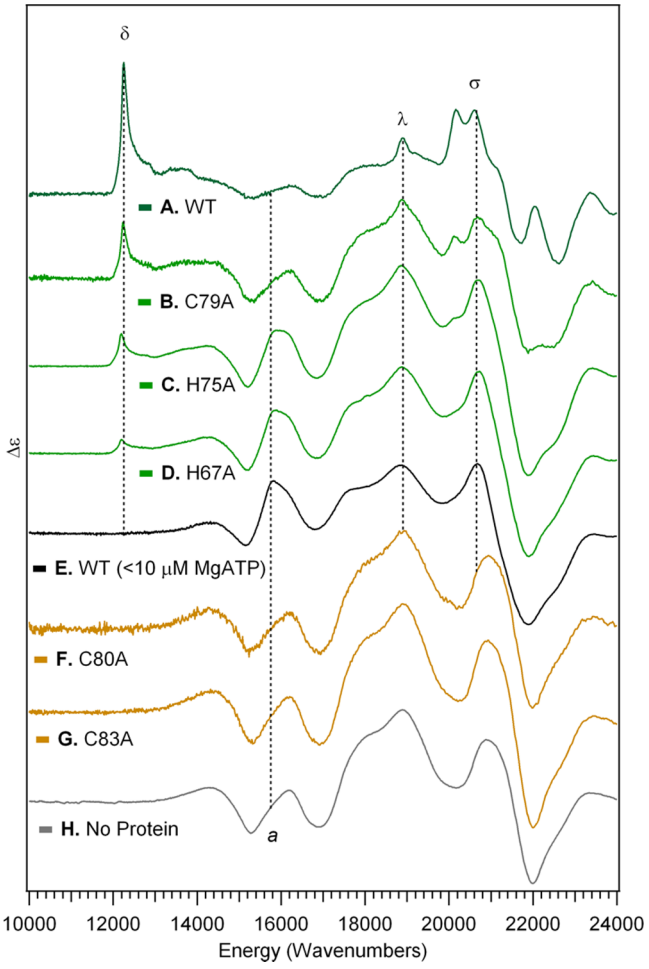

Figure 7. MCD spectra of Co(II)Cbl obtained in the presence of EutT^{WT}/Fe and selected variants (with >5 mM MgATP unless otherwise noted). The primary spectroscopic features due to 4c Co(II)Cbl species in the presence of EutT^{WT}/Fe (A) are highlighted by dashed vertical lines. Additional spectroscopic changes in reference to Co(II)Cbl in the absence of protein (H) are also highlighted.

H75A variant was included in this study because we initially assumed that residue His75 was part of the conserved divalent metal ion binding motif and the imidazole side chain of this residue could potentially coordinate to the divalent metal ion). While the spectra of Co(II)Cbl in the presence of EutT^{C80A}/Fe and EutT^{C83A}/Fe only contain features from 5c Co(II)Cbl, those obtained with EutT^{C79A}/Fe, EutT^{H67A}/Fe, and EutT^{H75A}/Fe additionally contain contributions from 4c Co(II)Cbl. However, as judged on the basis of the relative intensities of the MCD features associated with the 4c fraction of Co(II)Cbl, the 5c → 4c Co(II)Cbl conversion yields achieved by these latter variants are lower than that observed for EutT^{WT}/Fe. Overall, the 5c → 4c Co(II)Cbl conversion yields correlate well with the degree of Fe(II) incorporation into these variants as determined previously by elemental analysis, which revealed that EutT^{C80A} and EutT^{C83A} bind negligible amounts of Fe(II), while EutT^{C79A} and EutT^{H67A} incorporate ∼50% less Fe(II) than the wild-type enzyme. However, from these data alone it remained unclear if the alanine substitutions of residues within the $HX_{11}CCX_2C(83)$ motif cause a decrease in the 5c → 4c Co(II)Cbl conversion yield by suppressing Co(II)Cbl binding to the enzyme active site or by impeding the removal of the DMB moiety from the Co(II) ion.

The MCD spectra of Co(II)Cbl in the presence of EutT^{C80A}/Fe and EutT^{C83A}/Fe are virtually superimposable on that of free Co(II)Cbl (Figure 7), lacking any features attributable to base-off Co(II)Cbl. This observation indicates that both the EutT^{C80A}/Fe and the EutT^{C83A}/Fe variants do not bind Co(II)Cbl. In contrast, the MCD spectrum of Co(II)Cbl in the presence of EutT^{C79A}/Fe contains qualitatively similar, though considerably smaller contributions from 4c Co(II)Cbl as the spectrum obtained with EutT^{WT}/Fe. Despite the modest fraction of 4c Co(II)Cbl generated by this variant (about 50% of EutT^{WT}/Fe), the characteristic features from 4c Co(II)Cbl can be readily distinguished from those associated with 5c Co(II)Cbl species. Removal of the 4c Co(II)Cbl contributions to this MCD spectrum (via subtraction of the properly scaled spectrum of 4c Co(II)Cbl in the presence of EutT^{WT}/Fe) results in a spectrum that is essentially superimposable on that of free Co(II)Cbl (Figure S8), indicating that the remaining Co(II)Cbl fraction is not bound to the enzyme. Thus, the 50% decrease in the 5c → 4c Co(II)Cbl conversion yield in response to the C79A substitution likely stems from the ∼50% decrease in Fe(II) incorporation, as the Fe(II)-bound fraction of the protein appears capable of generating a similar 4c Co(II)Cbl species as EutT^{WT}/Fe. These findings indicate that C79 is not critical for maintaining the structure of the active site to the same degree as are the C80 and C83 residues, in particular with regards to the binding of Co(II)Cbl and the removal of the DMB moiety. In support of this conclusion, EutT^{C79A}/Fe has been found to be nearly as active as EutT^{WT}/Fe. It is therefore not surprising that residue C79 is not conserved among the known EutT ACATs.

A detailed analysis of the MCD spectra of Co(II)Cbl in the presence of EutT^{H67A}/Fe and EutT^{H75A}/Fe (Figures S9 and S10) reveals that these variants produce a significant fraction of base-off Co(II)Cbl, which is responsible for the features at ∼16 000 and ∼20 600 cm^{-1}. Moreover, the presence of base-off Co(II)Cbl in these variants is evidenced by the apparent red-shift of the feature observed at ∼16 300 cm^{-1} (Figure 7, feature *a*). The absence of a feature at 21 000 cm^{-1} shows that no base-on Co(II)Cbl remains unbound in solution, while the low intensity of the δ band at ∼12 000 cm^{-1} indicates that only a small fraction of 4c Co(II)Cbl is formed in the active sites of these variants. EPR data obtained for samples prepared under the same conditions confirm the presence of base-off and 4c Co(II)Cbl species, but also contain sizable contributions from base-on Co(II)Cbl (Figure S4). Because these spectra are very similar to that obtained with EutT^{WT}/Fe (except for differences in relative intensities due to variations in the different Co(II)Cbl populations) and the corresponding MCD spectra

DOI: 10.1021/jacs.5b11708
J. Am. Chem. Soc. 2016, 138, 3694−3704

indicate that all species are enzyme-bound, we conclude that the Co(II)Cbl binding motif of the enzyme is not disrupted by the H75A and H67A substitutions. However, since these substitutions cause an increase in the relative populations of enzyme-bound base-off and base-on Co(II)Cbl species at the expense of the 4c Co(II)Cbl fraction, residues H75 and H67 appear to play a role in the mechanism of 4c Co(II)Cbl formation by promoting axial ligand dissociation from 5c Co(II)Cbl either directly or indirectly by enhancing the degree of Fe(II) and Zn(II) incorporation into EutT.

DISCUSSION

The EutT^{WT} Active Site Promotes DMB Dissociation to Generate Base-Off Co(II)Cbl. As shown in this study, the combined use of MCD and EPR spectroscopies is well suited to characterize the base-off, base-on, and 4c Co(II)Cbl species generated in the EutT^{WT} active site and to determine their relative populations. Our EPR data indicate that in the presence of EutT^{WT} and substoichiometric MgATP, as much as 60% of Co(II)Cbl is present in the base-off conformation. Nevertheless, we have recently shown that EutT^{WT}/Zn binds Co(II)Cbi^{+} very weakly and is unable to adenoslyate this naturally occurring base-off Co(II)Cbl analogue.[41] Additionally, we observed small but significant differences between the MCD spectra of free Co(II)Cbi^{+} and the EutT^{WT}/Zn-bound base-off Co(II)Cbl species. These findings led us to propose that specific interactions between certain amino acid residues and the nucleotide loop are required to produce base-off Co(II)Cbl in the enzyme active site.[41] These interactions could introduce changes to the conformation of the corrin ring, especially in the region of C(17) that serves as the anchor of the nucleotide loop (Figure 1), as well as alter the environment around the H_2O ligand in base-off Co(II)Cbl, both of which could contribute to the small MCD and EPR spectral differences that exist between free and enzyme-bound base-off Co(II)Cbl. A more constrained conformation of the corrin ring of the base-off Co(II)Cbl species generated in the EutT^{WT} active site would also explain the observation of resolved hyperfine structure in the g_x region of the corresponding EPR spectrum (Figure 4). Similarly, the slight differences between the MCD and EPR spectra of the base-on Co(II)Cbl species bound to EutT^{WT} and free Co(II)Cbl could arise from enzyme-induced structural perturbations to the corrin ring prior to DMB dissociation. A constrained corrin ring conformation may be a critical prerequisite for the removal of the DMB ligand from the Co(II) ion, as otherwise the Co(II)Cbl substrate could simply reorient in response to external forces acting on the nucleotide loop.

Nature of the 4c Co(II)Cbl Species Generated in the EutT Active Site. The 4c Co(II)Cbl species generated in the active sites of other ACATs such as *Lr*PduO and *Se*CobA exhibit large (~600 to ~800 MHz) cobalt hyperfine coupling parameters, A(Co), consistent with a high degree of localization of the unpaired spin density on the Co(II) ion in the absence of axial ligands. The unusually large g-shifts from the free-electron value of 2.0023 displayed by these species ($g_x \approx g_y \gg g_z \sim 2.0$) have been shown to reflect an increase in the extent of spin−orbit mixing between the ground state and LF excited states due to a large stabilization of the Co $3d_{z^2}$-based MO in this conformation.[36,37] To this end, it is interesting to note that the 4c Co(II)Cbl species generated in the active site of EutT^{WT} displays a rhombic g-tensor ($g_x > g_y > g_z$) with the largest g spread and A(Co) values observed for any Co(II)rrinoid characterized to date (Table 2). While these results provide compelling evidence that the 4c Co(II)Cbl species generated in the EutT^{WT} active site adopts a unique conformation, it is difficult to interpret the corresponding g- and A-values in terms of specific structural perturbations because a proper description of the electronic structure of this species requires the use of wave function-based multireference techniques and a non-perturbative approach for the calculation of spin−orbit coupling effects.[40] The available crystal structures for *Lr*PduO and *Se*CobA in the presence of Co(II)Cbl and MgATP show that the corrin ring of the 4c Co(II)Cbl species generated in these enzymes adopts a planar conformation in which the four nitrogen atoms have become nearly symmetry-equivalent.[33,34] A computational analysis of 4c Co(II)Cbl indicated that in this species the unpaired spin density is localized in an MO that also has sizable contributions from orbitals other than the Co $3d_{z^2}$ orbital. In the case of 4c Co(II)Cbl generated in the EutT^{WT} active site, the large difference between the g_x and g_y values indicates that the Co $3d_{xz}$- and Co $3d_{yz}$-based MOs have substantially different energies, consistent with a nonplanar conformation of the corrin ring. A perturbed conformation of the corrin ring could also explain the largely red-shifted α-band observed in the Abs spectrum of this species, as the corrin π^*-based HOMO that serves as the donor orbital for this transition contains small contributions from the Co $3d_{xz}$ and Co $3d_{yz}$ orbitals.[36]

Another intriguing difference between the 4c Co(II)Cbl species formed in the EutT^{WT} active site and those observed in the presence of other ACATs is the large difference in intensity of the δ-band at ~12 000 cm^{-1} in the corresponding MCD spectra (Figure 2A). Even in the presence of a >50-fold molar excess of MgATP, conditions under which complete conversion to 4c Co(II)Cbl should occur, the MCD intensity of the δ-band remains less than 0.22 mM^{-1} cm^{-1} for all EutT samples studied. For the 4c Co(II)Cbl species formed in the active sites of *Se*CobA and *Lr*PduO, the intensity of this feature was previously estimated to be 0.505 mM^{-1} cm^{-1} (by accounting for the relative populations of 4c and 5c Co(II)Cbl). The lower MCD intensity of the δ-band in the spectrum of 4c Co(II)Cbl generated in the active site of EutT species remains puzzling,[41] but likely reflects the uniquely perturbed conformation of the 4c Co(II)Cbl substrate bound to this enzyme.

Comparison of the Co(II) → Co(I)Cbl Conversion Mechanisms of Known ACATs. In all ACATs studied to date, the redox tuning of the Co(II)Cbl substrate required for the formation of the essential Co(I)Cbl intermediate is achieved by inducing a complete dissociation of the axially bound DMB ligand to generate a square planar 4c Co(II)-rrinoid species that can be readily reduced by intracellular reducing agents (Figure 8).[26] In the case of *Lr*PduO, X-ray crystallographic studies revealed that the side chains of residues F112, F187, and V186 form a hydrophobic "wall" upon binding of Co(II)Cbl and MgATP, serving to block solvent access to the Coα face of the corrin ring, and a salt bridge interaction between D35 and R128 near the corrin ring binding site was found to be critical for promoting the dissociation of the DMB moiety.[35,38] A similar mechanism was proposed for *Se*CobA, where residues F91 and W93 were found to be important for generating 4c Co(II)rrinoids and for properly positioning the Co(I) intermediate that is subsequently formed during turnover.[33,39] However, the differences in the specific architectures of these active sites have an effect on the relative populations of 4c Co(II)rrinoids that are being formed.

DOI: 10.1021/jacs.5b11708
J. Am. Chem. Soc. 2016, 138, 3694−3704

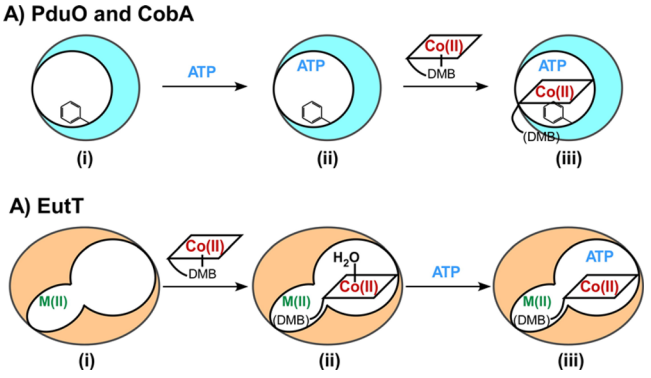

Figure 8. Proposed mechanisms for the formation of 4c Co(II)Cbl employed by the different ACAT families. In the case of the PduO- and CobA-type ACATs (A), spectroscopic and kinetic studies[3,37−39] revealed that the substrate-free enzyme (i) must first bind ATP (ii) before it can bind Co(II)Cbl. Crystal structures of the tertiary complex[33−35] (iii) provided evidence that in both enzymes a conserved phenylalanine residue blocks the position originally occupied by the DMB moiety in free Co(II)Cbl. In these structures the DMB moiety is unresolved, which argues against the presence of a specific nucleotide binding pocket as expected on the basis of the fact that these enzymes can adenosylate both Co(II)Cbl and Co(II)Cbi$^+$. In the case of EutT, the results obtained in the present study indicate that Co(II)Cbl can bind to the enzyme active site in the absence of ATP (i) to form a base-off Co(II)Cbl species in which a water molecule is presumably bound in the upper axial position (ii). In this binary complex, the DMB moiety is sequestered in a pocket lined by residues of the $HX_{11}CCX_2C(83)$ motif whose architecture changes in response to Fe(II) or Zn(II) ion binding. The subsequent binding of ATP to the enzyme active site triggers the dissociation of the axially bound water molecule to form 4c Co(II)Cbl (iii). Note that our data do not rule out the possibility that in the case of EutT the order of substrate binding is unimportant.

Although *Se*CobA and *Lr*PduO achieve very similar relative yields of 4c Co(II)Cbi$^+$ species (~50%), *Lr*PduO is able to generate ~40% of 4c Co(II)Cbl while in the case of *Se*CobA this yield is decreased to ~8%.[36,37,39] The higher 5c → 4c conversion yields for Co(II)Cbi$^+$ compared to Co(II)Cbl have generally been attributed to the weaker axial bond in Co(II)Cbi$^+$ and the fact that a higher level of coordination among different active site residues is required to remove the DMB moiety from the Co(II) ion of Co(II)Cbl.[38] From this perspective, it is rather unusual that EutT^{WT} can only adenoslylate Co(II)Cbl, and not Co(II)Cbi$^+$. Although previous studies revealed that Co(II)Cbi$^+$ does bind to the EutT^{WT} active site, albeit weakly, the axially bound water ligand is retained in this process.[41]

The results obtained in the present study indicate that binding of Co(II)Cbl to the EutT^{WT} active site and the formation of a large population of a 5c base-off species occur even in the absence of MgATP. This is in stark contrast to the ordered binding scheme observed for *Se*CobA and *Lr*PduO, where ATP must bind first for the enzyme to adopt a conformation suitable for binding of Co(II)rrinoids (Figure 8A).[3,33,34] However, 4c Co(II)Cbl is generated only in the presence of an excess of cosusbtrate MgATP, with higher concentrations resulting in higher yields. These observations suggest a mechanism for EutT^{WT} in which the active site forms a unique base-off Co(II)Cbl species prior to MgATP incorporation that serves as a precursor to 4c Co(II)Cbl (Figure 8B). As removal of the H_2O ligand is more facile than removal of the DMB moiety, the formation of a base-off intermediate should facilitate the formation of 4c Co(II)Cbl, which would explain the high 5c → 4c yield observed for EutT^{WT} (>95% for EutT^{WT}/Fe + MgATP). In this proposed mechanism, specific residues in the enzyme active site serve to lock the corrin ring in place, giving rise to the unique spectroscopic features observed experimentally, with additional protein motifs sequestering the DMB moiety away from the Co(II) ion (Figure 8B). In the case of Co(II)Cbi$^+$, the absence of the nucleotide loop and terminal DMB moiety prevent the active site from adopting the proper conformation needed for the formation of a 4c Co(II)Cbi$^+$ species in response to MgATP binding near the Coβ face of the corrin ring. Given that Co(II)Cbi$^+$ has been found to bind to EutT much less tightly than Co(II)Cbl, it is plausible that the former can respond to MgATP binding to the active site simply by repositioning itself without loss of the axial ligand. In the case of enzyme-bound 5c base-off Co(II)Cbl, MgATP binding to the active site in a position suitable to react with the subsequently formed Co(I)Cbl intermediate could trigger the dissociation of an axially bound water molecule on the Coβ face of the corrin ring (Figure 8B), thereby permitting the enzyme to control the timing of Co(I)Cbl formation and suppress the likelihood of undesired side-reactions by this "supernucleophile". While the specific amino acid residues used to stabilize enzyme-bound 5c base-off and 4c Co(II)Cbl species remain unknown in the absence of a crystal structure of EutT, it is tempting to speculate that the divalent metal site and $HX_{11}CCX_2C(83)$ motifs are involved in the removal of the DMB moiety, and thus are important for 4c Co(II)Cbl formation. Studies of Co(II)-substituted EutT, aimed at elucidating the structure of this metal site and evaluating its role in the catalytic cycle of EutT, will be presented elsewhere.

■ ASSOCIATED CONTENT

Supporting Information

The Supporting Information is available free of charge on the ACS Publications website at DOI: 10.1021/jacs.5b11708.

Details about compositions of all samples used in this study, additional low-temperature Abs, MCD, and EPR spectra of Co(II)Cbl in the presence of EutT^{WT}/Zn, EutT^{WT}/Fe, and selected variants under various conditions, and Gaussian deconvolutions of the MCD spectra of Co(II)Cbl obtained in the presence of several EutT/Fe variants (PDF)

■ AUTHOR INFORMATION

Corresponding Author

*brunold@chem.wisc.edu

Notes

The authors declare no competing financial interest.

■ ACKNOWLEDGMENTS

This work was supported in part by the National Science Foundation Grants MCB-238530 (to T.C.B.) and CHE-0840494. I.G.P. was supported in part by Grant 5T32GM08349 via the Biotechnology Training Grant at UW-Madison. T.C.M was supported in part by the National Institutes of Health Grant T32 GM008505 (Chemistry and Biology Interface Training Grant) and by the National Institutes of Health Grant R37-GM40313 to J.C.E.-S.

DOI: 10.1021/jacs.5b11708
J. Am. Chem. Soc. 2016, 138, 3694−3704

REFERENCES

(1) Sheppard, D. E.; Penrod, J. T.; Bobik, T.; Roth, J. R.; Kofoid, E. *J. Bacteriol.* **2004**, *186* (22), 7635−7644.
(2) Buan, N. R.; Suh, S.; Escalante-Semerena, J. C. *J. Bacteriol.* **2004**, *186* (17), 5708−5714.
(3) Mera, P. E.; Escalante-Semerena, J. C. *Appl. Microbiol. Biotechnol.* **2010**, *88* (1), 41−48.
(4) Stich, T. A.; Brooks, A. J.; Buan, N. R.; Brunold, T. C. *J. Am. Chem. Soc.* **2003**, *125* (19), 5897−5914.
(5) Conrad, K. S.; Brunold, T. C. *Inorg. Chem.* **2011**, *50* (18), 8755−8766.
(6) Pallares, I. G.; Brunold, T. C. *Inorg. Chem.* **2014**, *53* (14), 7676−7691.
(7) Stich, T. A.; Buan, N. R.; Brunold, T. C. *J. Am. Chem. Soc.* **2004**, *126* (31), 9735−9749.
(8) Mori, K.; Bando, R.; Hieda, N.; Toraya, T. *J. Bacteriol.* **2004**, *186* (20), 6845−6854.
(9) Banerjee, R.; Ragsdale, S. W. *Annu. Rev. Biochem.* **2003**, *72*, 209−247.
(10) Yeates, T. O.; Crowley, C. S.; Tanaka, S. *Annu. Rev. Biophys.* **2010**, *39*, 185−205.
(11) Chowdhury, C.; Sinha, S.; Chun, S.; Yeates, T. O.; Bobik, T. A. *Microbiol. Mol. Biol. Rev.* **2014**, *78* (3), 438−468.
(12) Kerfeld, C. A.; Heinhorst, S.; Cannon, G. C. *Annu. Rev. Microbiol.* **2010**, *64*, 391−408.
(13) Sampson, E. M.; Bobik, T. A. *J. Bacteriol.* **2008**, *190* (8), 2966−2971.
(14) Thiennimitr, P.; Winter, S. E.; Winter, M. G.; Xavier, M. N.; Tolstikov, V.; Huseby, D. L.; Sterzenbach, T.; Tsolis, R. M.; Roth, J. R.; Baumler, A. J. *Proc. Natl. Acad. Sci. U. S. A.* **2011**, *108* (42), 17480−17485.
(15) Garsin, D. A. *Nat. Rev. Microbiol.* **2010**, *8* (4), 290−295.
(16) Shibata, N.; Tamagaki, H.; Hieda, N.; Akita, K.; Komori, H.; Shomura, Y.; Terawaki, S.-I.; Mori, K.; Yasuoka, N.; Higuchi, Y.; Toraya, T. *J. Biol. Chem.* **2010**, *285* (34), 26484−26493.
(17) Buan, N. R.; Escalante-Semerena, J. C. *J. Biol. Chem.* **2006**, *281* (25), 16971−16977.
(18) Tsoy, O.; Ravcheev, D.; Mushegian, A. *J. Bacteriol.* **2009**, *191* (23), 7157−7164.
(19) Warren, M. J.; Raux, E.; Schubert, H. L.; Escalante-Semerena, J. C. *Nat. Prod. Rep.* **2002**, *19* (4), 390−412.
(20) Escalante-Semerena, J. C.; Suh, S. J.; Roth, J. R. *J. Bacteriol.* **1990**, *172* (1), 273−280.
(21) Jorge-Finnigan, A.; Aguado, C.; Sánchez-Alcudia, R.; Abia, D.; Richard, E.; Merinero, B.; Gámez, A.; Banerjee, R.; Desviat, L. R.; Ugarte, M.; Pérez, B. *Hum. Mutat.* **2010**, *31* (9), 1033−1042.
(22) Padovani, D.; Labunska, T.; Palfey, B. A.; Ballou, D. P.; Banerjee, R. *Nat. Chem. Biol.* **2008**, *4* (3), 194−196.
(23) Fonseca, M. V.; Escalante-Semerena, J. C. *J. Bacteriol.* **2000**, *182* (15), 4304−4309.
(24) Liptak, M. D.; Brunold, T. C. *J. Am. Chem. Soc.* **2006**, *128* (28), 9144−9156.
(25) Faure, D.; Lexa, D.; Savéant, J.-M. *J. Electroanal. Chem. Interfacial Electrochem.* **1982**, *140* (2), 297−309.
(26) Mera, P. E.; Escalante-Semerena, J. C. *J. Biol. Chem.* **2010**, *285* (5), 2911−2917.
(27) Moore, T. C.; Mera, P. E.; Escalante-Semerena, J. C. *J. Bacteriol.* **2014**, *196* (4), 903−910.
(28) Buan, N. R.; Escalante-Semerena, J. C. *J. Biol. Chem.* **2005**, *280* (49), 40948−40956.
(29) Mayhe, S. G.; Foust, G. P.; Massey, V. *J. Biol. Chem.* **1969**, *244* (3), 803−810.
(30) Hoover, D. M.; Jarrett, J. T.; Sands, R. H.; Dunham, W. R.; Ludwig, M. L.; Matthews, R. G. *Biochemistry* **1997**, *36* (1), 127−138.
(31) Mera, P. E.; St. Maurice, M.; Rayment, I.; Escalante-Semerena, J. C. *Biochemistry* **2007**, *46* (48), 13829−13836.
(32) Fonseca, M. V.; Buan, N. R.; Horswill, A. R.; Rayment, I.; Escalante-Semerena, J. C. *J. Biol. Chem.* **2002**, *277* (36), 33127−33131.
(33) Moore, T. C.; Newmister, S. a.; Rayment, I.; Escalante-Semerena, J. C. *Biochemistry* **2012**, *51* (48), 9647−9657.
(34) St. Maurice, M.; Mera, P.; Park, K.; Brunold, T. C.; Escalante-Semerena, J. C.; Rayment, I. *Biochemistry* **2008**, *47* (21), 5755−5766.
(35) Mera, P. E.; St Maurice, M.; Rayment, I.; Escalante-Semerena, J. C. *Biochemistry* **2009**, *48* (14), 3138−3145.
(36) Stich, T. A.; Buan, N. R.; Escalante-Semerena, J. C.; Brunold, T. C. *J. Am. Chem. Soc.* **2005**, *127* (24), 8710−8719.
(37) Park, K.; Mera, P. E.; Escalante-Semerena, J. C.; Brunold, T. C. *Biochemistry* **2008**, *47* (34), 9007−9015.
(38) Park, K.; Mera, P. E.; Escalante-Semerena, J. C.; Brunold, T. C. *Inorg. Chem.* **2012**, *51*, 4482−4494.
(39) Pallares, I. G.; Moore, T. C.; Escalante-Semerena, J. C.; Brunold, T. C. *Biochemistry* **2014**, *53*, 7969−7982.
(40) Liptak, M. D.; Fleischhacker, A. S.; Matthews, R. G.; Telser, J.; Brunold, T. C. *J. Phys. Chem. B* **2009**, *113* (15), 5245−5254.
(41) Park, K.; Mera, P. E.; Moore, T. C.; Escalante-Semerena, J. C.; Brunold, T. C. *Angew. Chem., Int. Ed.* **2015**, *54* (24), 7158−7161.
(42) Buan, N. R.; Suh, S.; Escalante-Semerena, J. C. *Microbiology* **2004**, *186* (17), 5708−5714.
(43) Blommel, P. G.; Fox, B. G. *Protein Expression Purif.* **2007**, *55* (1), 53−68.
(44) Nilges, M. J. Thesis in Chemistry, University of Illinois, Urbana-Champaign, IL, 1979.
(45) Pratt, J. M. *Inorganic Chemistry of Vitamin B12*; Academic Press Inc: London, 1972.
(46) Brooks, A. J.; Vlasie, M.; Banerjee, R.; Brunold, T. C. *J. Am. Chem. Soc.* **2005**, *127* (47), 16522−16528.
(47) Stich, T. A.; Yamanishi, M.; Banerjee, R.; Brunold, T. C. *J. Am. Chem. Soc.* **2005**, *127* (21), 7660−7661.

DOI: 10.1021/jacs.5b11708
J. Am. Chem. Soc. 2016, 138, 3694−3704